

**CONTROL OF SYNCHRONOUS RELUCTANCE MOTOR DRIVE FOR
SOLAR PV ARRAY FED WATER PUMPING**

ANSHUL VARSHNEY



**DEPARTMENT OF ELECTRICAL ENGINEERING
INDIAN INSTITUTE OF TECHNOLOGY DELHI
SEPTEMBER 2022**

**CONTROL OF SYNCHRONOUS RELUCTANCE MOTOR DRIVE FOR
SOLAR PV ARRAY FED WATER PUMPING**

by

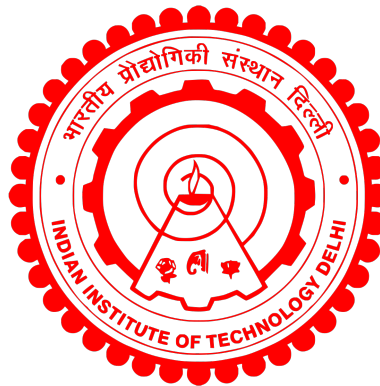
ANSHUL VARSHNEY

Department of Electrical Engineering

Submitted

in fulfillment of the requirements of the degree of DOCTOR OF PHILOSOPHY

to the



**Indian Institute of Technology Delhi
September 2022**

© Indian Institute of Technology Delhi (IITD), New Delhi, 2022

CERTIFICATE

This is to certify that the thesis entitled, “**Control of Synchronous Reluctance Motor Drive for Solar PV Array Fed Water Pumping**” being submitted by **Mr. Anshul Varshney** for the award of the degree of **Doctor of Philosophy** is a record of bonafide research work carried out by him in the Department of Electrical Engineering of Indian Institute of Technology Delhi.

Mr. Anshul Varshney has worked under my guidance and supervision and has fulfilled the requirements for the submission of this thesis, which to my knowledge has reached the requisite standard. The results obtained here in have not been submitted to any other University or Institute for the award of any degree.

Date:

Prof. Bhim Singh
Department of Electrical Engineering
Indian Institute of Technology Delhi,
New Delhi-110 016, India

ACKNOWLEDGEMENTS

Words cannot express my gratitude to my supervisor **Prof. Bhim Singh** for his invaluable patience and feedback. I could not have undertaken this journey without his guidance and constant supervision throughout my Ph.D. work. His keenness and vision have played an important role in guiding me throughout this study. I am indebted to **Prof. Bhim Singh** for the countless hours spent on discussions, thinking and proofreading of all my work. I am very grateful also to him that he is always very fast to replying to my queries. Working under him has been a wonderful experience, which has provided a deep insight to the world of research. Determination, dedication, innovativeness, resourcefulness and discipline of **Prof. Bhim Singh** have been the inspiration for me to complete this work. His consistent encouragement, continuous monitoring and commitments to excellence have always motivated me to improve my work and use the best of my capabilities.

My sincere thanks and deep gratitude are to all SRC Members, **Prof. Sukumar Mishra, Prof. Nilanjan Senroy, Prof. Ashu Verma** for their encouragement, insightful comments, expertise and hard questions.

I wish to convey my sincere thanks to Prof. Bhim Singh, Late Prof. M.L. Kothari, Prof. B.K. Panigrahi, Prof. Ramkrishan Maheshwari, Prof. Amit Kumar Jain for their valuable inputs during my course work, which made the foundation for my research work. I am grateful to IIT Delhi for providing me the research facilities. I would wish to express my sincere gratitude to Late Prof. K. R. Rajagopal, Prof. G. Bhuvaneshwari and Prof. M. Veerachary Prof. in-charge, PG Machines Lab., for providing me immense facilities to carry out experimental work. Thanks are due to Sh. Dhan Raj Singh, Sh. Srichand, Sh. Puran Singh, Sh. Jagbir Singh Shri Anurag, Shri Jitendra and Shri Amit Kumar of PG Machines Lab, UG Machines Lab and Power Electronics Lab., IIT Delhi for providing me the facilities and assistance during this work.

I would like to express my deepest appreciation to Dr. B. N. Singh, Dr. Sanjeet Dwivedi, Dr. Jeevanand, Dr. Ashish Srivastava, Dr. Sabha Raj Arya, Dr. V. Rajagopal and Dr. Ramnivas who always motivated me throughout my Ph.D. I am also grateful to Dr. Vashist Bist, Dr. Madishetti Sandeep, Dr. N. K. Swami Naidu, Dr. Chinmay Jain, Dr. Rajan Kumar and Dr. Ikhlq Hussain who have endorsed me during initial start-up of my research work. I would like to extend my sincere thanks to Dr. Sunil Kumar Pandey, Dr. Kanwar Pal, Dr. Subharni Pradhan, Dr. Subhra, Dr. Sreejith, Dr. Seema, Dr. Anjeet, Dr. Tabish, Dr. Deepu, Dr. Rahul Pandey, Dr. Piyush Kant, Dr.

Anjaneer, Dr. Sai Pranith, Dr. Aniket, Dr. Arun Kumar Verma, Dr. Geeta Pathak, Dr. Kapil Shukla, Dr. Rishi Sharma, Dr. Nikhil, Mr. Subir Karmakar, Dr. Neha Beniwal and Dr. Shailendra Tiwari for their valuable aid and co-operation. Many Thanks to Dr. Nishnat, Dr. Sachin, Dr. Saurabh, Ms. Shatakshi and Dr. Somnath for co-operation and informal support in pursuing experimental work. My deepest gratitude and sincere thanks are due to Dr. Shailendra Kumar and Dr. Utkarsh Sharma for their support in all the way throughout this work.

I thank my fellow labmates, Mr. Vineet P Chandaran, Mohammad Junaid, Mr. Gurmeet Singh, Ms. Vandana Jain, Mr. Debasish Mishra, Mr. Praveen Kumar Singh, Ms. Yashi Singh, Ms. Aakanksha, Ms. Sunaina Singh, Mr. Vardan Saxena, Mr. Niranjana Devela, Mr. G. K. Taneja, Mr. Khusro Khan, Ms. Rohini Sharma, Ms. Pavitra Shukl, Mr. Sambasivaiah, Dr. Priyank Shah, Dr. Neha Beniwal, Ms. Nupur, Ms. Hina Parveen, Ms. Jincy, Ms. Rashmi Rai, Mr. Yalavarthi Amarnath, Mr. Arayadip Sen, Mr. Kashif, Mr. Gaurav Modi, Mr. Sudip Bhattacharya, Mr. Bilal Naqvi, Mr. Jitendra Gupta, Mr. Sandeep Kumar Sahoo, Ms. Shalvi Tyagi, Mr. Souvik Das, Mr. Vivek Narayanan, Mr. Suri Praneeth, Mr. Priyvrata Vats, Mr. SayandeB Ghosh, Mr. Saran Chaurashiya, Mr. Sharan Shastri, Mr. Shivam Yadav, Mr. Rahul Kumar, Mr. Deepak Saw, Ms. Kousalya V, Ms. Chandrakala Devi, Mr. Saurabh Mishra, Mr. Girja Shankar, Mr. Zarkab, Ms. Kripa, Mr. Rohit, Mr. Vipin, Ms. Farha, Ms. Smita Mr. Himanshu Grover and all PG Machine lab group for their valuable support. for the stimulating discussions, for the sleepless nights we were working together before deadlines, and for all the fun we have had during my stay in PG Machines Lab. I also thank Mr. Yatindra, Mr. Satish, Mr. Sandeep and all other Electrical Engineering office staff for being supportive throughout. How could I forget my hostel mates Dr. Anup Kumar Mandpura, Dr. Somesh Bhattacharya and Dr. Anup Godiyal, who supported and inspired me during my stay in 'Jwalamukhi' hostel. I am likewise thankful to those who suffer directly or indirectly, helped me to finish my dissertation study.

I would like to offer my sincere thanks to Prof. A. S. Arora, Prof. Raj Kumar Garg and Prof. Sanjeev Singh who have given me motivation for pursuing Ph.D.

I would be remiss in not mentioning my friends, Dr. Sunil, Dr. Vivek, Dr. Harish, Dr. Bhuvnesh, Dr. Varun, Dr. R. K. Bera, Dr. Avni Khatkad and Mr. Unnikrishnan VT for their endless supports and guidance.

Blessings of my grandparents, Late Sh. Shivnandan Gupta and Late Smt. Prabhavati, have al-

ways strengthened me in my entire life. My deepest love and appreciation goes to my parents Mr. Rishabh Prakash Varshney and Mrs. Hemwati for their wholehearted support, patience, encouragement and valuable time sharing. I would like to thank my younger brother Ambuj Varshney and younger sister Mansi Varshney for their continuous support and encouragement. Their trust in my capabilities had been a key factor to all my achievements. Moreover, I would like to thank my wife Ms. Kajal Gupta for giving me the inner strength and wholehearted support.

Moreover, I would like to thank Department of Science and Technology (DST), Govt. of India for funding this research work under project grant number RP02926 (Intelligent Control of Solar Photovoltaic Array Fed Water Pumping Systems).

I offer my deep gratitude to the Director and colleagues of CSIR-National Physical Laboratory for supporting me during my Ph.D. program at IIT Delhi.

At last, I am beholden to almighty for their blessings to help me to raise my academic level to this stage. I pray for their benediction in my future endeavors. Their blessings may be showered on me for strength, wisdom and determination to achieve in future.

Date:

Anshul Varshney

ABSTRACT

This research work presents numerous topologies of a synchronous reluctance motor (SyRM) drive based solar PV array fed water pumping system. A SyRM is chosen because of its simple control, robustness and higher efficiency than other AC motors. The SyRM is characterized by the absence of rotor currents, which makes ideally the winding losses in the rotor zero. Therefore, the efficiency of the SyRM, is superior to than some other motors. It makes the drive control intelligible in comparison to an induction motor and permanent magnet motors. Thus, the use of SyRM for driving the pump and elimination of speed/position sensor, provide a unique solution for solar powered water pumping system.

In this work, an attempt has been made to develop solar photovoltaic array fed water pumping system with added features of grid interface. In standalone systems, single stage and two stage systems are implemented. Merits and demerits of both the systems are pointed out. For standalone system, reference speed is altered until maximum power point is reached as power drawn is proportional to the cube of the speed. In two stage system, a boost converter is utilized for harvesting maximum available power from a PV array through an incremental conductance based maximum power point tracking algorithm. Here, it feeds power to a voltage source inverter (VSI) through a DC link capacitor. DC link voltage is maintained to the reference value by adjusting the speed of the motor. However, in single stage system, only one power converter, i.e., VSI is required for MPPT as well as motor control. In case of grid connected single phase unidirectional topology, power factor correction (PFC) boost converter is used in continuous conduction mode (CCM). The pump is run at rated speed in case of availability of the grid at unity power factor while taking maximum available power from the solar PV array. As variable frequency drives draw nonlinear current, PFC boost converter reduces the total harmonics distortion (THD) of the current drawn to less than allowable limit of 5%. In case of grid failure, pump continues to run at available maximum power from the solar PV array. Grid connected three phase bidirectional power flow configuration using front end converter (FEC) is also designed and tested in the laboratory. Apart from the features of the unidirectional topology, here excess power from the solar PV array is fed to the grid. This is important from the electricity bill reduction point of view. Moreover single phase, bidirectional configuration is conceptualized and simulated. The prime objective of proposed system, is to provide water supply for domestic and irrigation purposes, therefore, to avoid

complexity and for increased reliability, the speed/position sensor is eliminated. A speed/position observer is utilized for the estimation of angular position of SyRM. A PV feed-forward term is used to estimate the reference speed, which aids in enhancing the transient behavior of proposed system. Moreover, the control is inherently resistant to the ageing related variation in pump's constant. In this work, the magnetic saturation and cross coupling effects are taken into consideration while estimating the position. The magnetic saturation effects on the position estimation in SyRM, because the position is estimated with the help of direct and quadrature axis flux linkages. The direct and quadrature axis flux linkages directly depend on direct and quadrature axis inductances. If magnetic saturation or cross coupling effect is not taken into consideration, the center of the circle plotted between direct and quadrature axis flux linkages, is shifted from the origin because of magnetic saturation and cross coupling effect. Due to this effect, a delay is introduced between actual position and estimated position. All the proposed topologies are modelled and simulated using MATLAB/Simulink platform in order to demonstrate their behaviour during starting, steady state and dynamic conditions. The validity of simulation results are verified through test results obtained from experimental setup developed in the laboratory. The applicability and commercial potential of proposed systems are justified by their in-depth analysis based on efficiency, cost, simplicity and performance.

सार

इस शोध कार्य में एक सिंक्रोनस रिलक्टेंस मोटर (एसवाईआरएम) ड्राइव आधारित सौर पीवी एरे फेड वाटर पम्पिंग सिस्टम की कई टोपोलॉजी प्रस्तुत की गई हैं। एक एसवाईआरएम को अन्य एसी मोटरों की तुलना में इसके सरल नियंत्रण, मजबूती और उच्च दक्षता के कारण चुना जाता है। एसवाईआरएम को रोटर धाराओं की अनुपस्थिति की विशेषता है, जिसके कारण रोटर वाइंडिंग में होने वाली हानि लगभग समाप्त हो जाती है, इसीलिए एसवाईआरएम की दक्षता कुछ अन्य मोटरों की तुलना में बेहतर है। यह इंडक्शन मोटर और परमानेंट मैग्नेट मोटर्स की तुलना में ड्राइव नियंत्रण को सुगम बनाता है। इस प्रकार, पंप चलाने के लिए एसवाईआरएम का उपयोग और गति / स्थिति सेंसर को समाप्त करना, सौर ऊर्जा संचालित जल पंपिंग प्रणाली के लिए एक अनूठा समाधान प्रदान करता है।

इस कार्य में ग्रिड इंटरफेस सिस्टम की अतिरिक्त विशेषताओं के साथ एक ऐसा सौर फोटोवोल्टिक एरे फेड वाटर पम्पिंग सिस्टम विकसित करने का प्रयास किया गया है, जिसमें ग्रिड इंटरफेस सिस्टम की अतिरिक्त विशेषताएँ हैं। स्टैंडअलोन सिस्टम में, सिंगल स्टेज और टू स्टेज सिस्टम लागू किए जाते हैं। दोनों प्रणालियों के गुण और दोष बताए गए हैं। स्टैंडअलोन सिस्टम के लिए, संदर्भ गति को तब तक बदल दिया जाता है जब तक कि अधिकतम पावर पॉइंट तक नहीं पहुंच जाता क्योंकि शक्ति गति के घन के आनुपातिक होती है। दो चरण प्रणाली में, एक इंक्रीमेंटल कन्डक्टन्स आधारित अधिकतम पावर प्वाइंट ट्रैकिंग एल्गोरिदम के माध्यम से एक पीवी एरे से अधिकतम शक्ति एक्सट्रेक्ट करने के लिए एक बूस्ट कन्वर्टर का उपयोग किया जाता है। यहां, यह डीसी लिंक कैपेसिटर के माध्यम से वोल्टेज स्रोत इन्वर्टर (वीएसआई) को पॉवर सप्लाय करता है। डीसी लिंक वोल्टेज मोटर की गति को समायोजित करके संदर्भ वैल्यू पर बनाए रखा जाता है। हालांकि, सिंगल स्टेज सिस्टम में, एमपीपीटी के साथ-साथ मोटर नियंत्रण के लिए केवल एक पावर कन्वर्टर यानी वीएसआई की आवश्यकता होती है। ग्रिड कनेक्टेड सिंगल फेज यूनिडायरेक्शनल टोपोलॉजी के मामले में, पावर फैक्टर करेक्शन (पीएफसी) बूस्ट कन्वर्टर का इस्तेमाल कंटीन्यूअस कंडक्शन मोड (सीसीएम) में किया जाता है। सोलर पीवी एरे से अधिकतम उपलब्ध बिजली लेते हुए यूनिटी पावर फैक्टर पर ग्रिड की उपलब्धता के मामले में पंप को रेटेड गति से चलाया जाता है। चूंकि वेरिएबल फ्रीक्वेंसी ड्राइव नॉनलाइनियर करंट खींचते हैं, पीएफसी बूस्ट कन्वर्टर वर्तमान के टोटल हार्मोनिक डिस्टॉर्शन (टी एच् डी) को 5% की स्वीकार्य सीमा से कम कर देता है। ग्रिड की विफलता के मामले में, सौर पीवी एरे से उपलब्ध अधिकतम शक्ति पर पंप चालू रहता है। फ्रंट एंड कन्वर्टर (एफईसी) का उपयोग करके ग्रिड से जुड़े थ्री फेज बाइडायरेक्शनल पॉवर फ्लो कण्ट्रोल आधारित सिस्टम को भी प्रयोगशाला में डिजाइन और परीक्षण किया गया है। यूनिडायरेक्शनल

टोपोलॉजी की विशेषताओं के अलावा, यहां सोलर पीवी ऐरे से अतिरिक्त पॉवर ग्रिड को फीड की जाती है। यह बिजली बिल में कमी की दृष्टि से महत्वपूर्ण है। इसके अलावा सिंगल फेज बाइडायरेक्शनल कॉन्फिगरेशन को कन्सेप्चुअलाइज़ और सिमुलेट किया गया है। प्रस्तावित प्रणाली का मुख्य उद्देश्य, घरेलू और सिंचाई उद्देश्यों के लिए पानी की आपूर्ति प्रदान करना है, इसलिए जटिलता से बचने के लिए और बढ़ी हुई विश्वसनीयता के लिए, गति/स्थिति सेंसर को समाप्त कर दिया जाता है। एसवाईआरएम की कोणीय स्थिति के आकलन के लिए एक गति/स्थिति पर्यवेक्षक का उपयोग किया जाता है। संदर्भ गति का अनुमान लगाने के लिए पीवी फीड-फॉरवर्ड टर्म का उपयोग किया जाता है, जो प्रस्तावित प्रणाली के क्षणिक व्यवहार को बढ़ाने में सहायता करता है। इसके अलावा, कण्ट्रोल पंप स्थिरांक में बदलाव का प्रतिरोधी है। इस कार्य में स्थिति का आकलन करते समय मैग्नेटिक सैचरेशन और क्रॉस कपलिंग प्रभावों को ध्यान में रखा जाता है। एसवाईआरएम में स्थिति के आकलन पर मैग्नेटिक सैचरेशन प्रभाव डालता है, क्योंकि स्थिति का अनुमान डायरेक्ट और क्राइचर अक्षों के फ्लक्स लिंकेज की सहायता से लगाया जाता है। डायरेक्ट और क्राइचर एक्सिस फ्लक्स लिंकेज सीधे डायरेक्ट और क्राइचर एक्सिस इंडक्शन पर निर्भर करते हैं। यदि मैग्नेटिक सैचरेशन या क्रॉस कपलिंग प्रभाव को ध्यान में नहीं रखा जाता है, तो मैग्नेटिक सैचरेशन और क्रॉस कपलिंग प्रभाव के कारण डायरेक्ट और क्राइचर एक्सिस फ्लक्स लिंकेज के बीच प्लॉट किए गए सर्कल के केंद्र को मूल से स्थानांतरित कर दिया जाता है। इस प्रभाव के कारण, वास्तविक स्थिति और अनुमानित स्थिति के बीच एक डिफेरेन्स आ जाता है। सभी प्रस्तावित टोपोलॉजी को मेटलैब/सिमुलिक प्लेटफॉर्म का उपयोग करके मॉडलिंग और सिमुलेट किया जाता है ताकि स्टार्टिंग, स्टेडी स्टेट और डायनामिक कंडीशन के दौरान उनके व्यवहार को प्रदर्शित किया जा सके। सिमुलेशन परिणामों की वैधता प्रयोगशाला में विकसित प्रयोगात्मक सेटअप से प्राप्त परीक्षण परिणामों के माध्यम से सत्यापित की जाती है। प्रस्तावित प्रणालियों की प्रयोज्यता और व्यावसायिक क्षमता दक्षता, लागत, सरलता और प्रदर्शन के आधार पर उनके गहन विश्लेषण द्वारा जस्टिफाई की गयी है।

TABLE OF CONTENTS

	Page
Certificate	i
Acknowledgments	iii
Abstract	vii
List of Figures	xxi
List of Abbreviations	xli
List of Symbols	xlili
CHAPTER - I INTRODUCTION	1
1.1 General	1
1.2 State of Art on Solar PV Fed Water Pumping	2
1.3 Objectives and Scope of Work	4
1.3.1 Standalone Solar PV Array Fed SyRM Drive for Water Pumping	5
1.3.2 Grid Conected Solar PV Based SyRM Drive for Water Pumping	6
1.4 Outline of Chapters	6
CHAPTER - II LITERATURE REVIEW	11
2.1 General	11
2.2 Literature Survey	12
2.2.1 History and Development of Solar PV Based Water Pumping Technology	13
2.2.2 Review of Solar PV Fed Water Pumping Systems	13
2.2.2.1 Solar PV Fed DC Motor Driven Water Pumping	14
2.2.2.2 Solar PV Fed Induction Motor Driven Water Pumping	14
2.2.2.3 Solar PV Fed BLDC Motor Driven Water Pumping	16
2.2.2.4 Solar PV Fed PMSM Driven Water Pumping	16
2.2.2.5 Solar PV Fed SRM Driven Water Pumping	17
2.2.2.6 Solar PV Fed SyRM Driven Water Pumping	17
2.2.2.7 Solar Energy Conversion Systems and Power Factor Correction	17
2.2.3 Review of MPPT Techniques for Solar PV Generation	18
2.2.4 Review of SyRM Drives for Solar PV fed Water Pumping	20
2.3 Identified Research Areas	21
2.4 Conclusions	22
CHAPTER - III STANDALONE TWO STAGE SOLAR PV FED SyRM DRIVE FOR WATER PUMPING	23
3.1 General	23

3.2	Configuration of Two Stage Standalone Solar PV Fed SyRM Drive for Water Pumping	23
3.3	Design of Two Stage Standalone Solar PV Fed SyRM Drive for Water Pumping	25
3.3.1	Design of Solar PV Array	25
3.3.2	Design of Boost Converter	26
3.3.3	Design of DC Bus Capacitor of VSI	26
3.3.4	Design of VSI	27
3.3.5	Design of Water Pump	27
3.4	Control of Two Stage Standalone Solar PV Fed SyRM Drive for Water Pumping	28
3.4.1	MPP Control of Solar PV Array with Boost Converter	29
3.4.2	Sensorless Speed Control of SyRM Drive	30
3.4.2.1	Constant d-axis Current Vector Control of SyRM Drive	35
3.4.2.2	Adaptive d-axis Current Vector Control of SyRM Drive	36
3.5	MATLAB Based Modeling and Simulation of Two Stage PV Fed SyRM Drive for Water Pumping	39
3.6	Hardware Implementation of Two Stage Standalone Solar PV Fed SyRM Drive for Water Pumping	39
3.6.1	Development of Interfacing Circuit for Voltage Sensors	42
3.6.2	Development of Interfacing Circuit for Current Sensors	42
3.6.3	Development of Isolation and Amplification Circuit for Gate Drivers	43
3.6.4	Real Time Execution of Control Algorithm on dSPACE 1202	44
3.7	Results and Discussion	46
3.7.1	Simulated performance of Constant d-axis Current Vector Control of SyRM Drive	46
3.7.1.1	Starting Performance	47
3.7.1.2	Steady State Performance	47
3.7.1.3	Dynamic Performance	49
3.7.2	Simulated performance of Adaptive d-axis Current Vector Control of SyRM Drive	51
3.7.2.1	Starting Performance	51
3.7.2.2	Steady State Performance	51
3.7.2.3	Dynamic Performance	54
3.7.3	Experimental Performance of Constant d-axis Current Vector Control of SyRM Drive	55
3.7.3.1	Starting Performance	56
3.7.3.2	Steady State Performance	59
3.7.3.3	Dynamic Performance	62

3.7.4	Experimental Performance of Adaptive d-axis Current Vector Control of SyRM Drive	63
3.7.4.1	Starting Performance	63
3.7.4.2	Steady State Performance	66
3.7.4.3	Dynamic Performance	68
3.8	Conclusions	70
CHAPTER - IV STANDALONE SINGLE STAGE SOLAR PV FED SyRM DRIVE FOR WATER PUMPING		73
4.1	General	73
4.2	Configuration of Single Stage Standalone Solar PV Fed SyRM Drive for Water Pumping	73
4.3	Design of Single Stage Standalone Solar PV Fed SyRM Drive for Water Pumping	75
4.3.1	Design of Solar PV Array	75
4.3.2	Design of DC Bus Capacitor of VSI	76
4.3.3	Design of VSI	76
4.3.4	Design of Water Pump	76
4.4	Control of Single Stage Standalone Solar PV Fed SyRM Drive for Water Pumping	76
4.4.1	MPP Control of Solar PV Array	77
4.4.2	Sensorless Speed Control of SyRM Drive	78
4.4.2.1	Constant d-axis Current Vector Control of SyRM Drive	79
4.4.2.2	Adaptive d-axis Current Vector Control of SyRM Drive	79
4.5	MATLAB Based Modelling and Simulation of Single Stage PV Fed SyRM Drive for Water Pumping	79
4.6	Hardware Implementation of Single Stage Standalone Solar PV Fed SyRM Drive for Water Pumping	81
4.7	Results and Discussion	81
4.7.1	Simulated performance of Constant d-axis Current Vector Control of SyRM Drive	81
4.7.1.1	Starting Performance	81
4.7.1.2	Steady State Performance	81
4.7.1.3	Dynamic Performance	82
4.7.2	Simulated performance of Adaptive d-axis Current Vector Control of SyRM Drive	82
4.7.2.1	Starting Performance	83
4.7.2.2	Steady State Performance	87
4.7.2.3	Dynamic Performance	87

4.7.3	Experimental Performance of Constant d-axis Current Vector Control of SyRM Drive	87
4.7.3.1	Starting Performance	90
4.7.3.2	Steady State Performance	91
4.7.3.3	Dynamic Performance	91
4.7.4	Experimental Performance of Adaptive d-axis Current Vector Control of SyRM Drive	92
4.7.4.1	Starting Performance	92
4.7.4.2	Steady State Performance	93
4.7.4.3	Dynamic Performance	95
4.8	Conclusions	100
 CHAPTER - V SINGLE PHASE GRID INTERFACED UNIDIRECTIONAL POWER FLOW CONTROL BASED TWO STAGE SOLAR PV FED SyRM DRIVE FOR WATER PUMPING		 103
5.1	General	103
5.2	Configuration and Operating Principle of Single-Phase Grid Interfaced Unidirectional Power Flow Control Based Two Stage Solar PV Fed SyRM Drive for Water Pumping	104
5.3	Design of Single-Phase Grid Interfaced Unidirectional Power Flow Control Based Two Stage Solar PV Fed SyRM Drive for Water Pumping	104
5.3.1	Design of Solar PV Array	105
5.3.2	Selection of DC Link Voltage and DC link Capacitor	105
5.3.3	Design of Boost Converter	106
5.3.4	Design of Grid Side Boost Converter	106
5.3.5	Design of Grid Side Filter	107
5.4	Control of Single-Phase Grid Interfaced Unidirectional Power Flow Control Based Two Stage Solar PV Fed SyRM Drive for Water Pumping	107
5.4.1	Maximum Power Point Tracking Algorithm	109
5.4.2	Control of Synchronous Reluctance Motor Drive	109
5.4.3	Power Factor Correction Technique	109
5.5	MATLAB Based Modelling and Simulation of Single-Phase Grid Interfaced Unidirectional Power Flow Control Based Two Stage Solar PV Fed SyRM Drive for Water Pumping	111
5.6	Hardware Implementation of Single-Phase Grid Interfaced Unidirectional Power Flow Control Based Two Stage Solar PV Fed SyRM Drive for Water Pumping	111
5.7	Results and Discussion	113

5.7.1	Simulated Performance	114
5.7.1.1	Performance When Water Pump is Fed by Solar PV Array Only	114
5.7.1.2	Performance When Water Pump is Fed by Grid Only	117
5.7.1.3	Performance When Water Pump is Fed by Solar PV Array and Grid	120
5.7.2	Experimental Performance	122
5.7.2.1	Performance When Water Pump is Fed by Solar PV Array Only	123
5.7.2.2	Performance When Water Pump is Fed by Grid Only	128
5.7.2.3	Performance When Water Pump is Fed by Solar PV Array and Grid	131
5.8	Conclusions	135
 CHAPTER - VI SINGLE PHASE GRID INTERFACED UNIDIRECTIONAL POWER FLOW CONTROL BASED SINGLE STAGE SOLAR PV FED SyRM DRIVE FOR WATER PUMPING		137
6.1	General	137
6.2	Configuration and Operating Principle of Single-Phase Grid Interfaced Unidirectional Power Flow Control Based Single Stage Solar PV Fed SyRM Drive for Water Pumping	138
6.3	Design of Single-Phase Grid Interfaced Unidirectional Power Flow Control Based Single Stage Solar PV Fed SyRM Drive for Water Pumping	139
6.3.1	Design of Solar PV Array	139
6.3.2	Selection of DC Link Voltage and DC link Capacitor	139
6.3.3	Design of Grid Side Boost Converter	139
6.3.4	Design of Grid Side Filter and Interfacing Inductor	139
6.4	Control of Single-Phase Grid Interfaced Unidirectional Power Flow Control Based Single Stage Solar PV Fed SyRM Drive for Water Pumping	140
6.4.1	Maximum Power Point Tracking Algorithm	140
6.4.2	Control of Synchronous Reluctance Motor Drive	140
6.4.3	Power Factor Correction Technique	141
6.5	MATLAB Based Modelling and Simulation of Single-Phase Grid Interfaced Unidirectional Power Flow Control Based Single Stage Solar PV Fed SyRM Drive for Water Pumping	141
6.6	Hardware Implementation of Single-Phase Grid Interfaced Unidirectional Power Flow Control Based Single Stage Solar PV Fed SyRM Drive for Water Pumping	142
6.7	Results and Discussion	143
6.7.1	Simulated Performance	145
6.7.1.1	Performance When Water Pump is Fed by Solar PV Array Only	145
6.7.1.2	Performance When Water Pump is Fed by Grid Only	147

6.7.1.3	Performance When Water Pump is Fed by Solar PV Array and Grid	150
6.7.2	Experimental Performance	154
6.7.2.1	Performance When Water Pump is Fed by Solar PV Array Only	154
6.7.2.2	Performance When Water Pump is Fed by Grid Only	158
6.7.2.3	Performance When Water Pump is Fed by Solar PV Array and Grid	162
6.8	Conclusions	168
CHAPTER - VII SINGLE PHASE GRID INTERFACED BIDIRECTIONAL POWER FLOW CONTROL BASED TWO STAGE SOLAR PV FED SyRM DRIVE FOR WATER PUMPING		169
7.1	General	169
7.2	Configuration and Operating Principle of Single-Phase Grid Interfaced Bidirectional Power Flow Control Based Two Stage Solar PV Fed SyRM Drive for Water Pumping	169
7.3	Design of Single-Phase Grid Interfaced Bidirectional Power Flow Control Based Two Stage Solar PV Fed SyRM Drive for Water Pumping	171
7.3.1	Design of Solar PV Array	171
7.3.2	Design of Boost Converter	171
7.3.3	Selection of DC Link Voltage and DC link Capacitor	171
7.3.4	Design of Interfacing Inductor	172
7.4	Control of Single-Phase Grid Interfaced Bidirectional Power Flow Control Based Two Stage Solar PV Fed SyRM Drive for Water Pumping	172
7.4.1	Maximum Power Point Tracking Algorithm	173
7.4.2	Control of Synchronous Reluctance Motor Drive	174
7.4.3	Bidirectional Power Flow Control	174
7.5	MATLAB Based Modelling and Simulation of Single-Phase Grid Interfaced Bidirectional Power Flow Control Based Two Stage Solar PV Fed SyRM Drive for Water Pumping	175
7.6	Hardware Implementation of Single-Phase Grid Interfaced Bidirectional Power Flow Control Based Two Stage Solar PV Fed SyRM Drive for Water Pumping	175
7.7	Results and Discussion	175
7.7.1	Simulated Performance	178
7.7.1.1	Performance When Water Pump is Fed by Solar PV Array Only	178
7.7.1.2	Performance When Water Pump is Fed by Grid Only	181
7.7.1.3	Performance When Water Pump is Fed by Solar PV Array and Grid	185
7.7.1.4	Performance When Solar PV Array Feeds Water Pump and Grid	187
7.7.2	Experimental Performance	189

7.7.2.1	Performance When Water Pump is Fed by Solar PV Array Only	191
7.7.2.2	Performance When Water Pump is Fed by Grid Only	196
7.7.2.3	Performance When Water Pump is Fed by Solar PV Array and Grid	197
7.7.2.4	Performance When Solar PV Array Feeds Water Pump and Grid	202
7.8	Conclusions	206

CHAPTER - VIII SINGLE PHASE GRID INTERFACED BIDIRECTIONAL POWER FLOW CONTROL BASED SINGLE STAGE SOLAR PV FED SyRM DRIVE FOR WATER PUMPING 209

8.1	General	209
8.2	Configuration and Operating Principle of Single-Phase Grid Interfaced Bidirectional Power Flow Control Based Single Stage Solar PV Fed SyRM Drive for Water Pumping	210
8.3	Design of Single-Phase Grid Interfaced Bidirectional Power Flow Control Based Single Stage Solar PV Fed SyRM Drive for Water Pumping	211
8.3.1	Selection of DC Link Voltage and DC link Capacitor	211
8.4	Control of Single-Phase Grid Interfaced Bidirectional Power Flow Control Based Single Stage Solar PV Fed SyRM Drive for Water Pumping	212
8.5	MATLAB Based Modelling and Simulation of Single-Phase Grid Interfaced Bidirectional Power Flow Control Based Single Stage Solar PV Fed SyRM Drive for Water Pumping	216
8.6	Hardware Implementation of Single-Phase Grid Interfaced Bidirectional Power Flow Control Based Single Stage Solar PV Fed SyRM Drive for Water Pumping	216
8.7	Results and Discussion	219
8.7.1	Simulated Performance	219
8.7.1.1	Performance When Water Pump is Fed by Solar PV Array Only	219
8.7.1.2	Performance When Water Pump is Fed by Grid Only	222
8.7.1.3	Performance When Water Pump is Fed by Solar PV Array and Grid	223
8.7.1.4	Performance When Solar PV Array Feeds Water Pump and Grid	227
8.7.2	Experimental Performance	229
8.7.2.1	Performance When Water Pump is Fed by Solar PV Array Only	231
8.7.2.2	Performance When Water Pump is Fed by Grid Only	236
8.7.2.3	Performance When Water Pump is Fed by Solar PV Array and Grid	239
8.7.2.4	Performance When Solar PV Array Feeds Water Pump and Grid	243
8.8	Conclusions	248

CHAPTER - IX THREE PHASE GRID INTERFACED BIDIRECTIONAL POWER FLOW CONTROL BASED TWO STAGE SOLAR PV FED SyRM

DRIVE FOR WATER PUMPING	249
9.1 General	249
9.2 Configuration and Operating Principle of Three-Phase Grid Interfaced Bidirectional Power Flow Control Based Two Stage Solar PV Fed SyRM Drive for Water Pumping	250
9.3 Design of Three-Phase Grid Interfaced Bidirectional Power Flow Control Based Two Stage Solar PV Fed SyRM Drive for Water Pumping	251
9.3.1 Selection of SyRM Power Rating	251
9.3.2 Design of Solar PV Array	252
9.3.3 Design of Boost Converter	252
9.3.4 Selection of DC link Capacitor	253
9.3.5 Design of Interfacing Inductor for VSC	253
9.4 Control of Three-Phase Grid Interfaced Bidirectional Power Flow Control Based Two Stage Solar PV Fed SyRM Drive for Water Pumping	254
9.4.1 Bi-directional Power Flow Control	254
9.4.2 Maximum Power Point Tracking Algorithm	257
9.4.3 Vector Control of SyRM Drive	257
9.4.4 Power Factor Correction Technique	260
9.5 MATLAB Based Modelling and Simulation of Three-Phase Grid Interfaced Bidirectional Power Flow Control Based Two Stage Solar PV Fed SyRM Drive for Water Pumping	262
9.6 Hardware Implementation of Three-Phase Grid Interfaced Bidirectional Power Flow Control Based Two Stage Solar PV Fed SyRM Drive for Water Pumping	262
9.7 Results and Discussion	265
9.7.1 Simulated Performance	265
9.7.1.1 Performance When Water Pump is Fed by Solar PV Array Only	265
9.7.1.2 Performance When Water Pump is Fed by Grid Only	267
9.7.1.3 Performance When Water Pump is Fed by Solar PV Array and Grid	272
9.7.1.4 Performance When Solar PV Array Feeds Water Pump and Grid	274
9.7.2 Experimental Performance	276
9.7.2.1 Performance When Water Pump is Fed by Solar PV Array Only	278
9.7.2.2 Performance When Water Pump is Fed by Grid Only	284
9.7.2.3 Performance When Water Pump is Fed by Solar PV Array and Grid	285
9.7.2.4 Performance When Solar PV Array Feeds Water Pump and Grid	288
9.8 Conclusions	293

CHAPTER - X	THREE PHASE GRID INTERFACED BIDIRECTIONAL POWER FLOW CONTROL BASED SINGLE STAGE SOLAR PV FED SyRM DRIVE FOR WATER PUMPING	295
10.1	General	295
10.2	Configuration and Operating Principle of Three-Phase Grid Interfaced Bidirectional Power Flow Control Based Single Stage Solar PV Fed SyRM Drive for Water Pumping	295
10.3	Design of Three-Phase Grid Interfaced Bidirectional Power Flow Control Based Single Stage Solar PV Fed SyRM Drive for Water Pumping	296
10.3.1	Design of Solar PV Array	297
10.3.2	Selection of DC Link Voltage and DC link Capacitor	297
10.3.3	Design of Interfacing Inductor and Grid Side Filter	297
10.4	Control of Three-Phase Grid Interfaced Bidirectional Power Flow Control Based Single Stage Solar PV Fed SyRM Drive for Water Pumping	297
10.4.1	Maximum Power Point Tracking Algorithm	298
10.4.2	Control of Synchronous Reluctance Motor Drive	298
10.4.3	Power Factor Correction Technique	298
10.5	MATLAB Based Modelling and Simulation of Three-Phase Grid Interfaced Bidirectional Power Flow Control Based Single Stage Solar PV Fed SyRM Drive for Water Pumping	299
10.6	Hardware Implementation of Three-Phase Grid Interfaced Bidirectional Power Flow Control Based Single Stage Solar PV Fed SyRM Drive for Water Pumping	299
10.7	Results and Discussion	302
10.7.1	Simulated Performance	302
10.7.1.1	Performance When Water Pump is Fed by Solar PV Array Only	302
10.7.1.2	Performance When Water Pump is Fed by Grid Only	305
10.7.1.3	Performance When Water Pump is Fed by Solar PV Array and Grid	308
10.7.1.4	Performance When Solar PV Array Feeds Water Pump and Grid	311
10.7.2	Experimental Performance	313
10.7.2.1	Performance When Water Pump is Fed by Solar PV Array Only	316
10.7.2.2	Performance When Water Pump is Fed by Grid Only	323
10.7.2.3	Performance When Water Pump is Fed by Solar PV Array and Grid	324
10.7.2.4	Performance When Solar PV Array Feeds Water Pump and Grid	328
10.8	Conclusions	332
CHAPTER - XI	MAIN CONCLUSIONS AND SUGGESTIONS FOR FURTHER WORK	335

11.1 General	335
11.2 Main Conclusions	336
11.3 Suggestion for Further Work	340
REFERENCES	342
APPENDICES	365
LIST OF PUBLICATIONS	369
BIO-DATA	373

LIST OF FIGURES

Fig. 1.1	Classification of solar PV array fed SyRM drive for water pumping system	5
Fig. 3.1	Configuration of two stage PV array fed water pumping system driven by synchronous reluctance motor	24
Fig. 3.2	Flow Chart for INC-MPPT algorithm	30
Fig. 3.3	Space Vector Diagram of SyRM	32
Fig. 3.4	Sensorless Speed Control Algorithm for SyRM Drive	34
Fig. 3.5	Constant d-axis Current Vector Control of SyRM Drive	36
Fig. 3.6	Adaptive d-axis Current Vector Control of SyRM Drive	38
Fig. 3.7	Matlab model of two stage PV fed SyRM drive for water pumping(a) Modelling of complete solar PV array fed water pumping system, (b) DC-DC Converter	40
Fig. 3.8	Matlab model of two stage PV fed SyRM drive for water pumping(a) Incremental Conductance based MPPT algorithm, (b) Vector Control Algorithm	41
Fig. 3.9	Laboratory prototype of developed SyRM drive based solar water pumping system	42
Fig. 3.10	Schematic of voltage sensor (a) Circuit of voltage sensor, (b) Voltage sensor board	43
Fig. 3.11	Schematic of current sensor (a) Circuit of current sensor, (b) Current sensor board	44
Fig. 3.12	Schematic of Opto-coupler circuit (a) Circuit of opto-coupler circuit, (b) Opto-coupler board	45
Fig. 3.13	Architecture of dSPACE-1202 (Microlab Box) (a) Execution of Control Algorithm (b) Microlab Box-1202	46
Fig. 3.14	Starting and steady state performance of the solar PV array	48
Fig. 3.15	Starting and steady state performance of boost converter	49
Fig. 3.16	Starting and steady state performance of SyRM-pump	50
Fig. 3.17	Dynamic Performance of Constant d-axis Current Vector Control of SyRM Drive for Two Stage Solar PV Array Fed Water Pumping System(a) Dynamic performance of solar PV array for increasing insolation, (b) Dynamic performance of SyRM-Pump for increasing insolation	52
Fig. 3.18	Dynamic Performance of Constant d-axis Current Vector Control of SyRM Drive for Two Stage Solar PV Array Fed Water Pumping System (a) Dynamic performance of solar PV array for decreasing insolation, (b) Dynamic performance of SyRM-Pump for decreasing insolation	53

Fig. 3.19	Starting and steady state performance of the solar PV array	54
Fig. 3.20	Starting and steady state performance of boost converter	55
Fig. 3.21	Starting and steady state performance of SyRM-pump	56
Fig. 3.22	Dynamic Performance of Adaptive d-axis Current Vector Control of SyRM Drive for Two Stage Solar PV Array Fed Water Pumping System(a) Dynamic performance of solar PV array for increasing insolation, (b) Dynamic performance of SyRM-Pump for increasing insolation	57
Fig. 3.23	Dynamic Performance of Adaptive d-axis Current Vector Control of SyRM Drive for Two Stage Solar PV Array Fed Water Pumping System (a) Dynamic performance of solar PV array for decreasing insolation, (b) Dynamic performance of SyRM-Pump for decreasing insolation	58
Fig. 3.24	Starting performance of the SyRM drive based two stage solar powered water pumping system	59
Fig. 3.25	Performance Indices of PV array (a) MPP performance at $1000W/m^2$ (b) MPP performance at $500W/m^2$	60
Fig. 3.26	Steady state response of PV array (a) at $1000W/m^2$, (b) at $500W/m^2$	60
Fig. 3.27	Steady state response of the system at $1000W/m^2$ (a) Boost converter parameter (b) Steady state performance of SyRM drive (c) Internal signals of the proposed system (ψ_d , ψ_q , ψ and θ), (d) Estimated signal of the system (T_e , ψ , I_a and N_r)	61
Fig. 3.28	Recorded internal signal of the proposed algorithm at $1000W/m^2$ (a) α, β axis voltage and current ($v_\alpha, v_\beta, i_\alpha, i_{beta}$) (b) DC link voltage and switching signals (c) SyRM drive estimated parameters (ψ_s, N_{ref}, N_{est} and L_d)	62
Fig. 3.29	Dynamic response of the system at $1000W/m^2$ (a) PV array performance for change in insolation from $1000W/m^2$ to $500W/m^2$ (b) from $500W/m^2$ to $1000W/m^2$ (c) SyRM drive estimated parameters for change in insolation from $1000W/m^2$ to $500W/m^2$ (d) SyRM drive estimated parameters for change in insolation from $500W/m^2$ to $1000W/m^2$	64
Fig. 3.30	Starting performance of SyRM drive based two stage solar powered water pumping system (a) Starting response at $1000W/m^2$ ($V_{pv}, I_{pv}, V_{dc}, I_a$) (b) Starting response at $1000W/m^2$ ($I_a, I_b, N_{est}, V_{dc}$) (c) Starting response at $1000W/m^2$ ($L_d, \gamma_\lambda, i_d, \lambda$) (d) Starting response at $1000W/m^2$, (T_e, θ, P_{pv}, D) (e) Starting response at $1000W/m^2$, ($V_\alpha, V_\beta, I_\alpha, I_\beta$)	65
Fig. 3.31	Performance Indices of PV array (a) MPP performance at $1000W/m^2$ (b) MPP performance at $500W/m^2$	66

Fig. 3.32 Steady state performance of solar water pumping system at $1000W/m^2$ (a) Steady state performance at $1000W/m^2$ ($V_{pv}, I_{pv}, V_{dc}, I_a$)(b) Steady state performance at $1000W/m^2$ (D, P_{pv}, T_e, N_{est})(c) Internal signals of the SyRM at $1000W/m^2$ ($i_d, i_q, \lambda_d, \lambda_q$) (d) Internal signals of the SyRM for reference speed calculation at $1000W/m^2$ (e) Reference currents and actual motor currents in dq- reference frame for steady state condition (f) Reference currents and actual motor currents for steady state condition (g) Internal signals of the real time d-axis inductance estimation algorithm (h) Estimated flux and torque for speed estimation (i) Internal signals of the sensorless speed assessment algorithm ($V_{dc}, V_\alpha, V_\beta, \theta$) 67

Fig. 3.33 Dynamic performance of the solar water pumping system for change in solar irradiation from $1000W/m^2$ to $500W/m^2$ (a) Dynamic performance for change in solar irradiation from $1000W/m^2$ to $500W/m^2$ ($V_{pv}, I_{pv}, V_{dc}, I_a$),(b) Dynamic performance for change in solar irradiation from $1000W/m^2$ to $500W/m^2$ ($P_{pv}, N_{est}, i_d, i_q$),(c) Dynamic performance for change in solar irradiation from $1000W/m^2$ to $500W/m^2$ ($V_{pv}, V_{dc}, N_{ref}, N_{est}$), (d) Internal signals of the SyRM for reference speed calculation for transients, (e) Reference currents and actual motor currents in dq- reference frame for transient, (f) Reference currents and actual motor currents for transient, (g) Internal signals of the real time d-axis inductance estimation algorithm, (h) Internal signals of the sensorless speed assessment algorithm ($V_{dc}, V_\alpha, V_\beta, \theta$), (i) Estimated flux and torque for speed estimation 69

Fig. 3.34 Dynamic performance of solar water pumping system for change in solar irradiation from $1000W/m^2$ to $500W/m^2$ (a) Dynamic performance for change in solar irradiation from $1000W/m^2$ to $500W/m^2$ ($V_{pv}, I_{pv}, V_{dc}, I_a$)(b) Dynamic performance for change in solar irradiation from $1000W/m^2$ to $500W/m^2$ ($P_{pv}, N_{est}, i_d, i_q$)(c) Dynamic performance for change in solar irradiation from $1000W/m^2$ to $500W/m^2$ ($V_{pv}, V_{dc}, N_{ref}, N_{est}$) (d) Internal signals of the SyRM for reference speed calculation for transients (e) Reference currents and actual motor currents in dq- reference frame for transient (f) Reference currents and actual motor currents for transient (g) Internal signals of the real time d-axis inductance estimation algorithm (h) Internal signals of the sensorless speed assessment algorithm ($V_{dc}, V_\alpha, V_\beta, \theta$) (i) Estimated flux and torque for speed estimation 70

Fig. 4.1 Single Stage Standalone Solar PV Fed SyRM Drive for Water Pumping 75

Fig. 4.2	Flow Chart of INC-MPPT Algorithm for Single Stage Standalone Solar PV Fed SyRM Drive for Water Pumping	77
Fig. 4.3	Matlab model of Single stage PV fed SyRM drive for water pumping(a) Modelling of complete single stage solar PV array fed water pumping system, (b) Single stage solar energy conversion system	80
Fig. 4.4	Starting and steady state performance of the solar PV array	82
Fig. 4.5	Starting and steady state performance of SyRM-pump	83
Fig. 4.6	Dynamic performance of single stage SyRM driven solar water pumping system for sudden decrease in insolation, (a) Solar PV array (b) SyRM-pump	84
Fig. 4.7	Dynamic performance of single stage SyRM driven solar water pumping system for sudden increase in insolation, (a) Solar PV array (b) SyRM-pump	85
Fig. 4.8	Starting and Steady State Performance of Single Stage Solar PV Array Fed Water Pumping System (a) Solar PV Array (b) SyRM and Pump	86
Fig. 4.9	Dynamic Performance of Single Stage Solar PV Array Fed Water Pumping System for change in insolation from $1000W/m^2$ to $500W/m^2$ (a) Solar PV array (b) SyRM-Pump	88
Fig. 4.10	Dynamic Performance of Single Stage Solar PV Array Fed Water Pumping System for change in insolation from $500W/m^2$ to $1000W/m^2$ (a) Solar PV array (b) SyRM-Pump	89
Fig. 4.11	Starting Performance of PV Array and SyRM-Pump	90
Fig. 4.12	Performance Indices of PV array (a) MPP performance at $1000W/m^2$, (b) MPP performance at $500W/m^2$	92
Fig. 4.13	Steady state response of solar water pumping system at $1000W/m^2$ (a) $(V_{pv}, I_{pv}, N_r, i_a)$ (b) (i_a, i_b, i_c, N_r) (c) Estimated signals of the motor ψ_d, ψ_q, ψ and θ (d) Flux hodograph of the SyRM	93
Fig. 4.14	Dynamic response of solar water pumping system for variation in insolation from $800W/m^2$ to $500W/m^2$ (a) $(V_{pv}, I_{pv}, N_r, i_a)$ (b) $(\psi_d, \psi_q, i_d, i_q)$ (c) $(V_{pv}, I_{pv}, N_r, i_a)$ (d) $(\psi_d, \psi_q, i_d, i_q)$	94
Fig. 4.15	Starting performance of single stage standalone solar water pumping system, (a) Starting performance of solar water pumping system $(V_{pv}, I_{pv}, I_m, N_r)$ at 100% solar insolation (b) Starting performance of solar water pumping system (I_a, I_b, I_c, N_r) at 100% solar insolation (c) Starting performance of solar water pumping system $(i_d, i_q, \lambda, \theta)$ at 100% solar insolation	95

Fig. 4.16	Performance Indices of PV array (a) MPP performance at $1000W/m^2$ (b) MPP performance at $500W/m^2$	96
Fig. 4.17	Steady state performance of single stage standalone solar water pumping system, (a) $(V_{pv}, I_{pv}, P_{pv}, I_m, N_r)$ at 100% solar insolation (b) Reference and actual SyRM currents (c) Reference and actual DC link voltage, Reference and estimated SyRM speed (d) Internal signal of control algorithm $(\psi_\alpha, \psi_\beta, i_d, i_q)$ (e) Internal signal of control algorithm (ψ, T_e, θ, L_d)	97
Fig. 4.18	Dynamic performance of single stage standalone solar water pumping system for change in insolation from $1000W/m^2$ to $600W/m^2$ (a) $(V_{pv}, I_{pv}, I_m, N_r)$ (b) $(V_{ref}, V_{pv}, N_{ref}, N_{est})$ (c) $(\psi_\alpha, \psi_\beta, \psi)$ (d) $(V_\alpha, V_\beta, i_\alpha, i_\beta)$	98
Fig. 4.19	Dynamic performance of single stage standalone solar water pumping system for change in insolation from $600W/m^2$ to $1000W/m^2$ (a) $(V_{pv}, I_{pv}, I_m, N_r)$ (b) $(V_{ref}, V_{pv}, N_{ref}, N_{est})$ (c) $(\psi_\alpha, \psi_\beta, \psi)$ (d) $(V_\alpha, V_\beta, i_\alpha, i_\beta)$	99
Fig. 4.20	Centre shifted flux and corrected flux	99
Fig. 4.21	Variation in the internal parameters of SyRM for change in insolation (a) Internal parameters of SyRM for change in insolation from $1000W/m^2$ to $600W/m^2$ (L_d, i_d, i_q, T_e) (b) Internal parameters of SyRM for change in insolation from $600W/m^2$ to $1000W/m^2$ (L_d, i_d, i_q, T_e)	100
Fig. 5.1	Configuration of the single phase grid interfaced unidirectional power flow control based two stage solar PV fed SyRM driven water pumping system	105
Fig. 5.2	Unidirectional power flow control scheme with power factor correction	111
Fig. 5.3	Single phase grid interfaced unidirectional power flow control based two stage solar PV fed SyRM drive for water pumping (a) Single phase grid interfaced unidirectional power flow control based two stage solar PV fed SyRM drive for water pumping (b) Power factor correction	112
Fig. 5.4	Unidirectional power flow control scheme with power factor correction	113
Fig. 5.5	Simulated performance of system at starting when water pump is fed by solar PV array only	115
Fig. 5.6	Simulated performance of system at steady state condition when water pump is fed by solar PV array only	116
Fig. 5.7	Simulated dynamic performance of system with decrease in solar radiation when water pump is fed by solar PV array only	117
Fig. 5.8	Simulated dynamic performance of system with increase in solar radiation when water pump is fed by solar PV array only	118
Fig. 5.9	Simulated performance of system at starting when water pump is fed by grid supply only	119

Fig. 5.10	Simulated performance of system at steady state condition when water pump is fed by grid supply only	120
Fig. 5.11	Simulated harmonic spectrum of supply current at AC mains when water pump is fed by grid supply only	121
Fig. 5.12	Simulated performance of system at steady state condition when water pump is fed by solar PV array and grid supply	122
Fig. 5.13	Simulated harmonic spectrum of supply current at AC mains when water pump is fed by solar PV array and grid supply only	123
Fig. 5.14	Simulated dynamic performance of the system when water pump is fed by solar PV array and grid supply	124
Fig. 5.15	Performance Indices of PV array (a) MPP performance at $500W/m^2$,(b) MPP performance at $1000W/m^2$	125
Fig. 5.16	Starting performance of single-phase grid interfaced unidirectional power flow control based two stage solar PV fed SyRM drive for water pumping system at $1000W/m^2$, (a) $V_{PV}, I_{PV}, P_{PV}, i_a$ and N_r , (b) V_{PV}, I_{PV}, V_{DC} and i_a , (c) V_{DC}, i_a, i_b and i_c	125
Fig. 5.17	Steady state performance of single-phase grid interfaced unidirectional power flow control based two stage solar PV fed SyRM drive for water pumping system at $1000W/m^2$ (a) $V_{PV}, I_{PV}, P_{PV}, i_a$ and N_r (b) D, P_{PV}, T_e and θ (c) V_{DC}, i_a, i_b and i_c (d) i_{aref}, i_a, N_{ref} and N_r (e) ψ_d, ψ_q, ψ and θ (f) L_d, i_q, V_{DC} and P_{PV}	127
Fig. 5.18	Transient performance of single-phase grid interfaced unidirectional power flow control based two stage solar PV fed SyRM drive for water pumping system for change in insolation from $1000W/m^2$ to $600W/m^2$ (a) $V_{PV}, I_{PV}, P_{PV}, i_a$ and N_r (b) V_{DC}, i_a, i_b and i_c (c) i_{aref}, i_a, N_{ref} and N_r (d) D, P_{PV}, T_e and θ (e) L_d, i_q, V_{DC} and P_{PV}	129
Fig. 5.19	Transient performance of single-phase grid interfaced unidirectional power flow control based two stage solar PV fed SyRM drive for water pumping system for change in insolation from $600W/m^2$ to $1000W/m^2$ (a) $V_{PV}, I_{PV}, P_{PV}, i_a$ and N_r (b) V_{DC}, i_a, i_b and i_c (c) i_{aref}, i_a, N_{ref} and N_r (d) D, P_{PV}, T_e and θ (e) L_d, i_q, V_{DC} and P_{PV}	130
Fig. 5.20	Starting performance of single-phase grid interfaced unidirectional power flow control based two stage solar PV fed SyRM drive for water pumping system with grid supply only (a) V_g, I_g, i_a and N_r (b) V_{DC}, i_a, i_b and i_c	131

Fig. 5.21	Steady state performance of single-phase grid interfaced unidirectional power flow control based two stage solar PV fed SyRM drive for water pumping system with grid supply only (a) V_g, I_g, i_a and N_r (b) V_g, I_g, V_{DC} and N_r (c) I_{Lgrid} and V_{sw} (d) D, I_g, θ and T_e	131
Fig. 5.22	Power Quality Parameters	132
Fig. 5.23	MPPT characteristics when water pump is fed by solar PV array and grid supply	132
Fig. 5.24	Steady state performance of single-phase grid interfaced unidirectional power flow control based two stage solar PV fed SyRM drive for water pumping system when fed by Solar PV Array and Grid Supply (a) V_g, I_g, P_{PV} and i_a (b) V_g, i_a, V_{DC} and P_{PV} (c) V_g, I_g, V_{PV}, I_{PV} and P_{PV} (d) V_g, I_g, T_e and θ	133
Fig. 5.25	Power quality parameters when water pump is fed by solar PV array and grid	134
Fig. 5.26	Transient performance of single-phase grid interfaced unidirectional power flow control based two stage solar PV fed SyRM drive for water pumping system for change in insolation from $1000W/m^2$ to $700W/m^2$ when fed by solar PV array and grid supply (a) V_g, I_g, P_{PV}, V_{PV} and I_{PV} (b) P_{PV}, D, I_g and N_r (c) $V_{PV}, I_{PV}, P_{PV}, V_{DC}$ and N_r (d) I_g, i_a, P_{PV} and V_{DC}	134
Fig. 5.27	Transient performance of single-phase grid interfaced unidirectional power flow control based two stage solar PV fed SyRM drive for water pumping system for change in insolation from $700W/m^2$ to $1000W/m^2$ when fed by solar PV array and grid supply (a) V_g, I_g, P_{PV}, V_{PV} and I_{PV} (b) P_{PV}, D, I_g and N_r (c) $V_{PV}, I_{PV}, P_{PV}, V_{DC}$ and N_r (d) I_g, i_a, P_{PV} and V_{DC}	135
Fig. 6.1	Configuration of single phase grid integrated single stage solar PV based SyRM driven water pumping system	138
Fig. 6.2	Unidirectional power flow control and vector control of SyRM	142
Fig. 6.3	Simulink model of single phase grid interfaced bidirectional power flow control based single stage solar PV fed SyRM drive for water pumping (Overall Simulink model and front end convertor control)	143
Fig. 6.4	Simulink model of single phase grid interfaced bidirectional power flow control based single stage solar PV fed SyRM drive for water pumping (MPPT Block and the pulse generation from the current controller block)	144
Fig. 6.5	Configuration of proposed system	145
Fig. 6.6	Simulated performance of system at starting when water pump is fed by solar PV array only	146
Fig. 6.7	Simulated performance of system at steady state condition when water pump is fed by solar PV array only	148

Fig. 6.8	Simulated dynamic performance of system with decrease in solar radiation when water pump is fed by solar PV array only	149
Fig. 6.9	Simulated dynamic performance of system with increase in solar radiation when water pump is fed by solar PV array only	150
Fig. 6.10	Simulated performance of system at starting when water pump is fed by grid supply only	151
Fig. 6.11	Simulated performance of the system at steady state condition when water pump is fed by grid supply only	152
Fig. 6.12	Simulated harmonic spectrum of supply current at AC mains when water pump is fed by grid supply only	152
Fig. 6.13	Simulated performance of system at steady state condition when water pump is fed by solar PV array and grid supply	153
Fig. 6.14	Simulated harmonic spectrum of supply current at AC mains when water pump is fed by solar PV array and grid supply only	154
Fig. 6.15	Simulated dynamic performance of system when water pump is fed by solar PV array and grid supply	155
Fig. 6.16	Performance Indices of PV array (a) MPP performance at $500W/m^2$ (b) MPP performance at $1000W/m^2$	156
Fig. 6.17	Starting performance of Single-Phase Grid Interfaced Unidirectional Power Flow Control Based Single Stage Solar PV Fed SyRM Drive for Water Pumping system at $1000W/m^2$ (a) $V_{PV}, I_{PV}, P_{PV}, i_a$ and N_r (b) V_{PV}, i_a, i_b and i_c	157
Fig. 6.18	Steady state performance of single-phase grid interfaced unidirectional power flow control based single stage solar PV fed SyRM drive for water pumping system at $1000W/m^2$ (a) $V_{PV}, I_{PV}, P_{PV}, i_a$ and N_r (b) V_{PV}, i_a, i_b and i_c (c) P_{PV}, T_e, θ and L_d (d) L_d, i_q, N_r and P_{PV} (e) ψ_d, ψ_q, ψ and θ (f) i_{aref}, i_a, N_{ref} and N_r	158
Fig. 6.19	Transient performance of single-phase grid interfaced unidirectional power flow control based single stage solar PV fed SyRM drive for water pumping system for change in insolation from $1000W/m^2$ to $500W/m^2$ (a) $V_{PV}, I_{PV}, P_{PV}, i_a$ and N_r (b) V_{PV}, i_a, i_b and i_c (c) P_{PV}, T_e, θ and L_d (d) L_d, i_q, N_r and P_{PV} (e) i_{aref}, i_a, N_{ref} and N_r	159
Fig. 6.20	Transient performance of single-phase grid interfaced unidirectional power flow control based single stage solar PV fed SyRM drive for water pumping system for change in insolation from $500W/m^2$ to $1000W/m^2$ (a) $V_{PV}, I_{PV}, P_{PV}, i_a$ and N_r (b) V_{PV}, i_a, i_b and i_c (c) P_{PV}, T_e, θ and L_d (d) L_d, i_q, N_r and P_{PV} (e) i_{aref}, i_a, N_{ref} and N_r	160

Fig. 6.21	Starting performance of single-phase grid interfaced unidirectional power flow control based single stage solar PV fed SyRM drive for water pumping system with grid supply only (a) V_g, I_g, i_a and N_r (b) V_{PV}, i_a, i_b and i_c	161
Fig. 6.22	Steady state performance of single-phase grid interfaced unidirectional power flow control based single stage solar PV fed SyRM drive for water pumping system with grid supply only (a) V_g, I_g, i_a and N_r (b) V_g, I_g, V_{DC} and N_r (c) V_{DC}, i_a, i_b and i_c (d) I_{Lgrid} and V_{sw} (e) D, I_g, θ and T_e	163
Fig. 6.23	Power quality parameters	164
Fig. 6.24	MPPT characteristics when water pump is fed by solar PV array and grid supply	164
Fig. 6.25	Steady state performance of single-phase grid interfaced unidirectional power flow control based single stage solar PV fed SyRM drive for water pumping system when fed by Solar PV Array and Grid Supply (a) V_g, I_g, P_{PV} and i_a (b) P_{PV}, I_g, i_a and N_r (c) $V_{PV}, I_{PV}, P_{PV}, N_r$ and I_g (d) D, i_a, I_g and N_r	165
Fig. 6.26	Power quality parameters when water pump is fed by solar PV array and grid	165
Fig. 6.27	Transient performance of single-phase grid interfaced unidirectional power flow control based single stage solar PV fed SyRM drive for water pumping system for change in insolation from $1000W/m^2$ to $500W/m^2$ when fed by solar PV array and grid supply (a) $V_{PV}, I_{PV}, P_{PV}, N_r$ and I_g (b) P_{PV}, I_g, i_a and N_r (c) V_g, I_g, T_e and θ , (d) L_d, i_q, N_r and P_{PV} (e) D, i_a, I_g and N_r	166
Fig. 6.28	Transient performance of single-phase grid interfaced unidirectional power flow control based single stage solar PV fed SyRM drive for water pumping system for change in insolation from $500W/m^2$ to $1000W/m^2$ when fed by solar PV array and grid supply (a) $V_{PV}, I_{PV}, P_{PV}, N_r$ and I_g (b) P_{PV}, I_g, i_a and N_r (c) V_g, I_g, T_e and θ (d) L_d, i_q, N_r and P_{PV} (e) D, i_a, I_g and N_r	167
Fig. 7.1	Configuration of single phase grid interfaced bidirectional power flow control based two stage solar PV fed SyRM driven water pumping system	170
Fig. 7.2	Control of Proposed System	174
Fig. 7.3	Simulink model of single phase grid interfaced bidirectional power flow control based single stage solar PV fed SyRM drive for water pumping (Overall Simulink model and front end convertor control)	176
Fig. 7.4	Simulink model of single phase grid interfaced bidirectional power flow control based single stage solar PV fed SyRM drive for water pumping (MPPT Block and the pulse generation from the current controller block)	177
Fig. 7.5	Simulated performance of system at starting when water pump is fed by solar PV array only	179

Fig. 7.6	Simulated performance of system at steady state condition when water pump is fed by solar PV array only	180
Fig. 7.7	Simulated dynamic performance of system with decrease in solar radiation when water pump is fed by solar PV array only	182
Fig. 7.8	Simulated dynamic performance of system with increase in solar radiation when water pump is fed by solar PV array only	183
Fig. 7.9	Simulated performance of system at starting when water pump is fed by grid supply only	184
Fig. 7.10	Simulated performance of the system at steady state condition when water pump is fed by grid supply only	185
Fig. 7.11	Simulated harmonic spectrum of supply current at AC mains when water pump is fed by grid supply only	186
Fig. 7.12	Simulated performance of system at steady state condition when water pump is fed by solar PV array and grid supply	187
Fig. 7.13	Simulated harmonic spectrum of supply current at AC mains when water pump is fed by solar PV array and grid supply only	188
Fig. 7.14	Simulated dynamic performance of system when water pump is fed by solar PV array and grid supply	189
Fig. 7.15	Simulated performance of system at steady state condition when solar PV array feeds water pump and grid	190
Fig. 7.16	Simulated harmonic spectrum of supply current at AC mains when solar PV array feeds water pump and grid	191
Fig. 7.17	Simulated dynamic performance of the system when solar PV array feeds water pump and grid	192
Fig. 7.18	Performance indices of PV array (a) MPP performance at $500W/m^2$ (b) MPP performance at $1000W/m^2$	193
Fig. 7.19	Starting performance of single-phase grid interfaced bidirectional power flow control based two stage solar PV fed SyRM drive for water pumping system at $500W/m^2$ (a) V_{PV}, I_{PV}, i_a and N_r (b) I_{PV}, V_{PV}, P_{PV} and N_r	194
Fig. 7.20	Steady state performance of single-phase grid interfaced bidirectional power flow control based two stage solar PV fed SyRM drive for water pumping system at $500W/m^2$ (a) $V_{PV}, I_{PV}, P_{PV}, i_a$ and N_r (b) V_{PV}, i_a, i_b and i_c (c) D, P_{PV}, T_e and θ (d) L_d, i_q, V_{DC} and P_{PV} (e) ψ_d, ψ_q, ψ and θ (f) i_{aref}, i_a, N_{ref} and N_r	195

Fig. 7.21	Transient performance of single-phase grid interfaced bidirectional power flow control based two stage solar PV fed SyRM drive for water pumping system for change in insolation from $500W/m^2$ to $250W/m^2$ (a) $V_{PV}, I_{PV}, P_{PV}, i_a$ and N_r (b) V_{DC}, i_a, i_b and i_c (c) $D, P_{PV}T_e$ and θ (d) L_d, i_q, V_{DC} and N_r (e) i_{aref}, i_a, N_{ref} and N_r	197
Fig. 7.22	Transient performance of single-phase grid interfaced bidirectional power flow control based two stage solar PV fed SyRM drive for water pumping system for change in insolation from $250W/m^2$ to $500W/m^2$ (a) $V_{PV}, I_{PV}, P_{PV}, i_a$ and N_r (b) V_{DC}, i_a, i_b and i_c (c) $D, P_{PV}T_e$ and θ (d) L_d, i_q, V_{DC} and N_r (e) i_{aref}, i_a, N_{ref} and N_r	198
Fig. 7.23	Starting performance of single-phase grid interfaced bidirectional power flow control based two stage solar PV fed SyRM drive for water pumping system with grid supply only (V_g, I_g, i_a and N_r)	199
Fig. 7.24	Steady state performance of single-phase grid interfaced bidirectional power flow control based two stage solar PV fed SyRM drive for water pumping system with grid supply only (a) V_g, I_g, i_a and N_r (b) V_g, I_g, V_{DC} and θ (c) V_g, I_g, T_e and θ (d) I_g, N_r, θ and i_a (e) ψ_d, ψ_q, ψ and θ ,	200
Fig. 7.25	Power quality parameters	201
Fig. 7.26	MPPT characteristics when water Pump is fed by solar PV array and grid supply	201
Fig. 7.27	Steady state performance of single-phase grid interfaced bidirectional power flow control based two stage solar PV fed SyRM drive for water pumping system at $275W/m^2$ (a) V_g, I_g, P_{PV} and i_a (b) $V_{PV}, I_{PV}, P_{PV}, V_{DC}$ and N_r	202
Fig. 7.28	Power quality parameters	202
Fig. 7.29	Transient performance of single-phase grid interfaced bidirectional power flow control based two stage solar PV fed SyRM drive for water pumping system for change in insolation from $500W/m^2$ to $200W/m^2$ (a) $V_{PV}, I_{PV}, P_{PV}, i_a$ and N_r (b) V_{DC}, I_g, P_{PV} and N_r	203
Fig. 7.30	Transient performance of single-phase grid interfaced bidirectional power flow control based two stage solar PV fed SyRM drive for water pumping system for change in insolation from $200W/m^2$ to $500W/m^2$ (a) $V_{PV}, I_{PV}, P_{PV}, i_a$ and N_r (b) V_{DC}, I_g, P_{PV} and N_r	203
Fig. 7.31	MPPT Characteristics when Solar PV Array Feeds Water Pump and Grid	204
Fig. 7.32	Steady state performance of single-phase grid interfaced bidirectional power flow control based two stage solar PV fed SyRM drive for water pumping system at $1000W/m^2$ (V_g, I_g, P_{PV} and i_a),	205

Fig. 7.33	Power quality parameters	205
Fig. 7.34	Transient performance of single-phase grid interfaced bidirectional power flow control based two stage solar PV fed SyRM drive for water pumping system for change in insolation from $800W/m^2$ to $300W/m^2$ (a) V_g, I_g, P_{PV} and i_a (b) V_g, I_g, T_e and N_r (c) L_d, i_q, P_{PV} and V_{DC} (d) V_{PV}, D, I_g and N_r	206
Fig. 8.1	Configuration of the single-phase grid interfaced bidirectional power flow control based single stage solar PV fed SyRM drive for water pumping system	211
Fig. 8.2	Control algorithm for SyRM and front-end converter	213
Fig. 8.3	Online estimation of d-axis inductance to compensate the effect of cross magnetization	215
Fig. 8.4	Simulink model of single phase grid interfaced bidirectional power flow control based single stage solar PV fed SyRM drive for water pumping (Overall Simulink model and front end convertor control)	217
Fig. 8.5	Simulink model of single phase grid interfaced bidirectional power flow control based single stage solar PV fed SyRM drive for water pumping (MPPT Block and the pulse generation from the current controller block)	218
Fig. 8.6	Simulated performance of system at starting when water pump is fed by solar PV array only	220
Fig. 8.7	Simulated performance of system at steady state condition when water pump is fed by solar PV array only	221
Fig. 8.8	Simulated dynamic performance of system with decrease in solar radiation when water pump is fed by solar PV array only	223
Fig. 8.9	Simulated dynamic performance of system with increase in solar radiation when water pump is fed by solar PV array only	224
Fig. 8.10	Simulated performance of system at starting when water pump is fed by grid supply only	225
Fig. 8.11	Simulated performance of system at starting when water pump is fed by grid supply only	226
Fig. 8.12	Simulated harmonic spectrum of supply current at AC mains when water pump is fed by grid supply only	227
Fig. 8.13	Simulated performance of system at steady state condition when water pump is fed by solar PV array and grid supply	228
Fig. 8.14	Simulated harmonic spectrum of supply current at AC mains when water pump is fed by solar PV array and grid supply only	229
Fig. 8.15	Simulated dynamic performance of system when water pump is fed by solar PV array and grid supply	230

Fig. 8.16	Simulated performance of system at steady state condition when solar PV array feeds water pump and grid	231
Fig. 8.17	Simulated harmonic spectrum of supply current at AC mains when solar PV array feeds water pump and grid	232
Fig. 8.18	Simulated dynamic performance of the system when solar PV array feeds water pump and grid	233
Fig. 8.19	Performance Indices of PV array (a) MPP performance at $500W/m^2$ (b) MPP performance at $1000W/m^2$	234
Fig. 8.20	Starting performance of single-phase grid interfaced bidirectional power flow control based single stage solar PV fed SyRM drive for water pumping system at $500W/m^2$ (a) $V_{PV}, I_{PV}, P_{PV}, i_a$ and N_r (b) V_{DC}, i_a, i_b and i_c	234
Fig. 8.21	Steady state performance of single-phase grid interfaced bidirectional power flow control based single stage solar PV fed SyRM drive for water pumping system at $500W/m^2$ (a) $V_{PV}, I_{PV}, P_{PV}, i_a$ and N_r (b) V_{DC}, i_a, i_b and i_c , (c) P_{PV}, T_e, θ and L_d (d) L_d, i_q, N_r and P_{PV} (e) ψ_d, ψ_q, ψ and θ (f) V_{ref}, V_{PV}, N_{ref} and N_r	236
Fig. 8.22	Transient performance of single-phase grid interfaced bidirectional power flow control based single stage solar PV fed SyRM drive for water pumping system for change in insolation from $500W/m^2$ to $250W/m^2$ (a) $V_{PV}, I_{PV}, P_{PV}, i_a$ and N_r (b) V_{DC}, i_a, i_b and i_c (c) V_{PV}, T_e, θ and L_d (d) L_d, i_q, N_r and P_{PV} (e) V_{ref}, V_{DC}, N_{ref} and N_r	237
Fig. 8.23	Transient performance of single-phase grid interfaced bidirectional power flow control based single stage solar PV fed SyRM drive for water pumping system for change in insolation from $500W/m^2$ to $250W/m^2$ (a) $V_{PV}, I_{PV}, P_{PV}, i_a$ and N_r (b) V_{DC}, i_a, i_b and i_c (c) V_{PV}, T_e, θ and L_d (d) L_d, i_q, N_r and P_{PV} (e) V_{ref}, V_{DC}, N_{ref} and N_r	238
Fig. 8.24	Starting performance of single-phase grid interfaced bidirectional power flow control based single stage solar PV fed SyRM drive for water pumping system with grid supply only (V_g, I_g, i_a and N_r)	239
Fig. 8.25	Steady state performance of single-phase grid interfaced bidirectional power flow control based single stage solar PV fed SyRM drive for water pumping system with grid supply only (a) V_g, I_g, i_a and N_r (b) i_a, i_b, i_c and N_r (c) I_g, N_r, θ and i_a (d) ψ_d, ψ_q, ψ and θ (e) V_g, I_g, T_e and L_d (f) V_g, I_g, V_{DC} and i_a ,	240
Fig. 8.26	Power quality parameters	241
Fig. 8.27	MPPT characteristics when water pump is fed by solar PV array and grid supply	241

Fig. 8.28	Steady state performance of single-phase grid interfaced bidirectional power flow control based single stage solar PV fed SyRM drive for water pumping system at $500W/m^2$ (a) $V_{PV}, I_{PV}, P_{PV}, i_a$ and N_r (b) V_g, I_g, P_{PV} and i_a	242
Fig. 8.29	Power quality parameters	242
Fig. 8.30	Transient performance of single-phase grid interfaced bidirectional power flow control based single stage solar PV fed SyRM drive for water pumping system for change in insolation from $250W/m^2$ to $500W/m^2$ (a) $V_{DC}, I_{PV}, P_{PV}, i_a$ and N_r (b) V_{DC}, I_g, P_{PV} and i_a (c) P_{PV}, I_g, V_g and N_r (d) V_g, I_g, V_{DC} and N_r (e) V_g, I_g, P_{PV} and i_a (f) L_d, i_q, N_r and P_{PV}	244
Fig. 8.31	Transient performance of single-phase grid interfaced bidirectional power flow control based single stage solar PV fed SyRM drive for water pumping system for change in insolation from $500W/m^2$ to $250W/m^2$ (a) $V_{DC}, I_{PV}, P_{PV}, i_a$ and N_r (b) V_{DC}, I_g, P_{PV} and i_a (c) P_{PV}, I_g, V_g and N_r (d) V_g, I_g, V_{DC} and N_r (e) V_g, I_g, P_{PV} and i_a (f) L_d, i_q, N_r and P_{PV}	245
Fig. 8.32	MPPT characteristics when solar PV array feeds water pump and grid	246
Fig. 8.33	Steady state performance of single-phase grid interfaced bidirectional power flow control based single stage solar PV fed SyRM drive for water pumping system at $1000W/m^2$ (V_g, I_g, P_{PV} and i_a),	246
Fig. 8.34	Power quality parameters	247
Fig. 8.35	Transient performance of single-phase grid interfaced bidirectional power flow control based single stage solar PV fed SyRM drive for water pumping system for change in insolation from $800W/m^2$ to $300W/m^2$ (V_g, I_g, P_{PV} and i_a)	247
Fig. 8.36	Transient performance of single-phase grid interfaced bidirectional power flow control based single stage solar PV fed SyRM drive for water pumping system for change in insolation from $300W/m^2$ to $800W/m^2$ (V_g, I_g, P_{PV} and i_a)	247
Fig. 9.1	Configuration of the three-phase grid interfaced bidirectional power flow control based two stage solar PV fed SyRM drive for water pumping system	251
Fig. 9.2	Speed control of SyRM and bidirectional power flow control	255
Fig. 9.3	Flow-chart for mode selection	256
Fig. 9.4	Space Vector Diagram of SyRM	260
Fig. 9.5	Simulink model of the single phase grid interfaced bidirectional power flow control based single stage solar PV fed SyRM drive for water pumping (Overall Simulink model and front end convertor control)	263
Fig. 9.6	Simulink model of the single phase grid interfaced bidirectional power flow control based single stage solar PV fed SyRM drive for water pumping (MPPT Block and the pulse generation from the current controller block)	264

Fig. 9.7	Simulated performance of system at starting when water pump is fed by solar PV array only	266
Fig. 9.8	Simulated performance of system at steady state condition when water pump is fed by solar PV array only	268
Fig. 9.9	Simulated dynamic performance of system with decrease in solar radiation when water pump is fed by solar PV array only	269
Fig. 9.10	Simulated dynamic performance of system with increase in solar radiation when water pump is fed by solar PV array only	270
Fig. 9.11	Simulated performance of system at starting when water pump is fed by grid supply only	271
Fig. 9.12	Simulated performance of system at starting when water pump is fed by grid supply only	272
Fig. 9.13	Simulated harmonic spectrum of supply current at AC mains when water pump is fed by grid supply only	273
Fig. 9.14	Simulated performance of system at steady state condition when water pump is fed by solar PV array and grid supply	274
Fig. 9.15	Simulated harmonic spectrum of supply current at AC mains when water pump is fed by solar PV array and grid supply only	275
Fig. 9.16	Simulated dynamic performance of system when water pump is fed by solar PV array and grid supply	276
Fig. 9.17	Simulated performance of system at steady state condition when solar PV array feeds water pump and grid	277
Fig. 9.18	Simulated harmonic spectrum of supply current at AC mains when solar PV array feeds water pump and grid	278
Fig. 9.19	Simulated dynamic performance of the system when solar PV array feeds water pump and grid	279
Fig. 9.20	Performance indices of PV array (a) MPP performance at $500W/m^2$ (b) MPP performance at $1000W/m^2$	280
Fig. 9.21	Starting performance of three-phase grid interfaced bidirectional power flow control based two stage solar PV fed SyRM drive for water pumping system at $500W/m^2$ (a) V_{PV}, I_{PV}, i_a and N_r (b) I_{PV}, P_{PV}, V_{DC} and i_a (c) D, P_{PV}, T_e and N_r	281
Fig. 9.22	Steady state performance of three-phase grid interfaced bidirectional power flow control based two stage solar PV fed SyRM drive for water pumping system at $500W/m^2$ (a) $V_{PV}, I_{PV}, P_{PV}, i_a$ and N_r (b) V_{DC}, i_a, i_b and i_c (c) ψ_d, ψ_q, ψ and θ (d) i_{aref}, i_a, N_{ref} and N_r (e) D, P_{PV}, T_e and θ	282

Fig. 9.23	Transient performance of three-phase grid interfaced bidirectional power flow control based two stage solar PV fed SyRM drive for water pumping system for change in insolation from $500W/m^2$ to $200W/m^2$ (a) $V_{PV}, I_{PV}, P_{PV}, i_a$ and N_r (b) V_{DC}, i_a, i_b and i_c (c) i_{aref}, i_a, N_{ref} and N_r (d) D, P_{PV}, T_e and θ	283
Fig. 9.24	Transient performance of three-phase grid interfaced bidirectional power flow control based two stage solar PV fed SyRM drive for water pumping system for change in insolation from $200W/m^2$ to $500W/m^2$ (a) $V_{PV}, I_{PV}, P_{PV}, i_a$ and N_r (b) V_{DC}, i_a, i_b and i_c (c) i_{aref}, i_a, N_{ref} and N_r (d) D, P_{PV}, T_e and θ	284
Fig. 9.25	Starting performance of three-phase grid interfaced bidirectional power flow control based two stage solar PV fed SyRM drive for water pumping system with grid supply only (V_g, I_g, i_a and N_r)	285
Fig. 9.26	Steady state performance of three-phase grid interfaced bidirectional power flow control based two stage solar PV fed SyRM drive for water pumping system with grid supply only (a) V_g, I_g, i_a and N_r (b) V_g, I_g, i_a and V_{DC}	286
Fig. 9.27	Power quality parameters	286
Fig. 9.28	MPPT Characteristics when Water Pump is Fed by Solar PV Array and Grid supply	287
Fig. 9.29	Steady state performance of three-phase grid interfaced bidirectional power flow control based two stage solar PV fed SyRM drive for water pumping system at $250W/m^2$ (a) V_g, I_g, P_{PV} and i_a (b) $V_{PV}, I_{PV}, P_{PV}, V_{DC}$ and N_r	287
Fig. 9.30	Power quality parameters	288
Fig. 9.31	Transient performance of three-phase grid interfaced bidirectional power flow control based two stage solar PV fed SyRM drive for water pumping system for change in insolation from $1000W/m^2$ to $500W/m^2$ (a) V_{PV}, I_{PV}, i_a and N_r (b) V_{DC}, I_g, P_{PV} and N_r	289
Fig. 9.32	Transient performance of three-phase grid interfaced bidirectional power flow control based two stage solar PV fed SyRM drive for water pumping system for change in insolation from $1000W/m^2$ to $500W/m^2$ (a) V_{PV}, I_{PV}, i_a and N_r (b) V_{DC}, I_g, P_{PV} and N_r	289
Fig. 9.33	MPPT Characteristics when Solar PV Array Feeds Water Pump and Grid	290
Fig. 9.34	Steady state performance of three-phase grid interfaced bidirectional power flow control based two stage solar PV fed SyRM drive for water pumping system at $1000W/m^2$ (V_g, I_g, P_{PV} and i_a),	290
Fig. 9.35	Power quality parameters	291

Fig. 9.36	Transient performance of three-phase grid interfaced bidirectional power flow control based two stage solar PV fed SyRM drive for water pumping system for change in insolation from $1000W/m^2$ to $700W/m^2$ (a) V_g, I_g, P_{PV} and i_a (b) V_g, I_g, V_{DC} and N_r (c) P_{PV}, D, I_g and N_r	291
Fig. 9.37	Transient performance of three-phase grid interfaced bidirectional power flow control based two stage solar PV fed SyRM drive for water pumping system for change in insolation from $700W/m^2$ to $1000W/m^2$ (a) V_g, I_g, P_{PV} and i_a (b) V_g, I_g, V_{DC} and N_r (c) P_{PV}, D, I_g and N_r	292
Fig. 9.38	Mode Transition Behaviour of Three-Phase Grid Interfaced Bidirectional Power Flow Control Based Two Stage Solar PV Fed SyRM Drive for Water Pumping system for change in insolation from $800W/m^2$ to $400W/m^2$ (a) V_g, i_g, P_{PV} and i_a (b) V_g, I_g, V_{DC} and N_r (c) P_{PV}, D, I_g and N_r	293
Fig. 10.1	Configuration of the three-phase grid interfaced bidirectional power flow control based single stage solar PV array fed SyRM drive for water pumping system	296
Fig. 10.2	Simulink model of single phase grid interfaced bidirectional power flow control based single stage solar PV fed SyRM drive for water pumping (Overall Simulink model and front end convertor control)	300
Fig. 10.3	Simulink model of single phase grid interfaced bidirectional power flow control based single stage solar PV fed SyRM drive for water pumping (MPPT Block and the pulse generation from the current controller block)	301
Fig. 10.4	Simulated performance of system at starting when water pump is fed by solar PV array only	303
Fig. 10.5	Simulated performance of system at steady state condition when water pump is fed by solar PV array only	304
Fig. 10.6	Simulated dynamic performance of system with decrease in solar radiation when water pump is fed by solar PV array only	306
Fig. 10.7	Simulated dynamic performance of system with increase in solar radiation when water pump is fed by solar PV array only	307
Fig. 10.8	Simulated performance of system at starting when water pump is fed by grid supply only	309
Fig. 10.9	Simulated performance of system at starting when water pump is fed by grid supply only	310
Fig. 10.10	Simulated harmonic spectrum of supply current at AC mains when water pump is fed by grid supply only	311

Fig. 10.11	Simulated performance of system at steady state condition when water pump is fed by solar PV array and grid supply	312
Fig. 10.12	Simulated harmonic spectrum of supply current at AC mains when water pump is fed by solar PV array and grid supply only	313
Fig. 10.13	Simulated dynamic performance of system when water pump is fed by solar PV array and grid supply	314
Fig. 10.14	Simulated performance of system at steady state condition when solar PV array feeds water pump and grid	315
Fig. 10.15	Simulated harmonic spectrum of supply current at AC mains when solar PV array feeds water pump and grid	316
Fig. 10.16	Simulated dynamic performance of the system when solar PV array feeds water pump and grid	317
Fig. 10.17	Performance indices of PV array (a) MPP performance at $500W/m^2$,(b) MPP performance at $1000W/m^2$	318
Fig. 10.18	Starting performance of three-phase grid interfaced bidirectional power flow control based single stage solar PV fed SyRM drive for water pumping system at $500W/m^2$ (a) V_{PV}, I_{PV}, i_a and N_r (b) V_{PV}, i_a, i_b and i_c	319
Fig. 10.19	Steady state performance of three-phase grid interfaced bidirectional power flow control based single stage solar PV fed SyRM drive for water pumping system at $500W/m^2$ (a) $V_{PV}, I_{PV}, P_{PV}, i_a$ and N_r (b) V_{PV}, i_a, i_b and i_c (c) V_{PV}, T_e, θ and N_r (d) ψ_d, ψ_q, ψ , and θ (e) L_d, i_q, N_r and P_{PV} (f) i_{aref}, i_a, N_{ref} and N_r	320
Fig. 10.20	Transient performance of three-phase grid interfaced bidirectional power flow control based single stage solar PV fed SyRM drive for water pumping system for change in insolation from $500W/m^2$ to $200W/m^2$ (a) $V_{PV}, I_{PV}, P_{PV}, i_a$ and N_r (b) V_{PV}, i_a, i_b and i_c	321
Fig. 10.21	Transient performance of three-phase grid interfaced bidirectional power flow control based single stage solar PV fed SyRM drive for water pumping system for change in insolation from $500W/m^2$ to $200W/m^2$ (a) V_{PV}, T_e, θ and N_r , (b) L_d, i_q, N_r and P_{PV} and θ (c) i_{aref}, i_a, N_{ref} and N_r	322
Fig. 10.22	Transient performance of three-phase grid interfaced bidirectional power flow control based single stage solar PV fed SyRM drive for water pumping system for change in insolation from $200W/m^2$ to $500W/m^2$ (a) $V_{PV}, I_{PV}, P_{PV}, i_a$ and N_r (b) V_{PV}, i_a, i_b and i_c	322

Fig. 10.23	Transient performance of three-phase grid interfaced bidirectional power flow control based single stage solar PV fed SyRM drive for water pumping system for change in insolation from $200W/m^2$ to $500W/m^2$ (a) V_{PV}, T_e, θ and N_r (b) L_d, i_q, N_r and P_{PV} and θ (c) i_{aref}, i_a, N_{ref} and N_r	323
Fig. 10.24	Starting performance of three-phase grid interfaced bidirectional power flow control based single stage solar PV fed SyRM drive for water pumping system with grid supply only (V_g, I_g, i_a and N_r)	324
Fig. 10.25	Steady state performance of three-phase grid interfaced bidirectional power flow control based single stage solar PV fed SyRM drive for water pumping system with grid supply only (a) V_g, I_g, i_a and N_r (b) V_g, I_g, V_{DC} and N_r (c) V_g, I_{ga}, I_{gb} and I_{gc} (d) V_g, I_g, i_a and θ	325
Fig. 10.26	Power quality parameters	325
Fig. 10.27	MPPT characteristics when water pump is fed by solar PV array and grid supply	326
Fig. 10.28	Steady state performance of three-phase grid interfaced bidirectional power flow control based single stage solar PV fed SyRM drive for water pumping system at $300W/m^2$ (a) $V_{PV}, I_{PV}, P_{PV}, N_r$ and I_g (b) V_g, I_g, P_{PV} and i_a	327
Fig. 10.29	Power quality parameters	327
Fig. 10.30	Transient performance of three-phase grid interfaced bidirectional power flow control based single stage solar PV fed SyRM drive for water pumping system for change in insolation from $700W/m^2$ to $300W/m^2$ (a) $V_{DC}, I_{PV}, P_{PV}, N_r$ and I_g (b) V_{DC}, i_g, P_{PV} and i_a (c) L_d, i_q, N_r and P_{PV}	328
Fig. 10.31	Transient performance of three-phase grid interfaced bidirectional power flow control based single stage solar PV fed SyRM drive for water pumping system for change in insolation from $300W/m^2$ to $700W/m^2$ (a) $V_{DC}, I_{PV}, P_{PV}, N_r$ and I_g (b) V_{DC}, i_g, P_{PV} and i_a (c) L_d, i_q, N_r and P_{PV}	329
Fig. 10.32	MPPT characteristics when solar PV array feeds water pump and grid	330
Fig. 10.33	Steady state performance of three-phase grid interfaced bidirectional power flow control based single stage solar PV fed SyRM drive for water pumping system at $1000W/m^2$ (V_g, I_g, P_{PV} and i_a),	330
Fig. 10.34	Power quality parameters	331
Fig. 10.35	Transient performance of three-phase grid interfaced bidirectional power flow control based single stage solar PV fed SyRM drive for water pumping system for change in insolation from $900W/m^2$ to $300W/m^2$ (a) P_{PV}, I_g, V_g and N_r (b) V_g, I_g, P_{PV} and i_a (c) V_g, I_g, V_{DC} and N_r	331

Fig. 10.36 Transient performance of three-phase grid interfaced bidirectional power flow control based single stage solar PV fed SyRM drive for water pumping system for change in insolation from $300W/m^2$ to $900W/m^2$ (a) P_{PV} , I_g , V_g and N_r (b) V_g , I_g , P_{PV} and i_a (c) V_g , I_g , V_{DC} and N_r

332

VSI	Voltage Source Inverter
SECS	Solar Energy Conversion System
DCM	Disconteneous Conduction Mode
IGBT	Insulated Gate Bipolar Transistor
MOSFET	Metal Oxide Semiconductor Field Effect Transistor
VFD	Variable Frequency Drive
MAF	Moving Average Filter
IC	Integrated Circuit
UPF	Unity Power Factor
LPF	Low Pass Filter

LIST OF ABBREVIATIONS

AC	Alternating Current
ADC	Analog to Digital Converter
ANN	Artificial Neural Network
ASD	Adjustable Speed Drives
BLDC	Brushless DC
CCM	Contineous Conduction Mode
DAC	Digital to Analog Converter
DC	Direct Current
DTC	Direct Torque Control
EMI	Electro-magnetic Interference
IM	Induction Motor
PMSM	Permanent Magnet Synchronous Motor
SRM	Switched Reluctance Motor
SyRM	Synchronous Reluctance Motor
FEC	Front End Converter
DSP	Digital Signal Processor
IEC	International Electrotechnical Commision
IEEE	Institute of Electrical and Electronics Engineers
INC	Incremental Conductance
MPP	Maximum Power Point
MPPT	Maximum Power Point Tracking
PCC	Point of Common Coupling
PFC	Power Factor Correction
PI	Proportional Integral
PLL	Phase Locked Loop
PV	Solar Photovoltaic
THD	Total Harmonic Distortion
VSC	Voltage Source Converter

LIST OF SYMBOLS

a	Over loading factor
C_{dc}	DC-link capacitor
C_f	Capacitor of the R-C ripple filter
C_{pv}	Capacitor across the PV array
D	Duty cycle of boost converter
P_{mpp}	MPP power
V_{mpp}	MPP power
I_{mpp}	MPP power
P_{PV}	PV array power
V_{PV}	PV array voltage
I_{PV}	PV array current
m	Modulation index
f_{sw}	Switching frequency of PV boost converter
θ_r	SyRM rotor angle
ρ_s	Angle of stator flux linkage space vector to the real-axis of the stator reference frame
δ_s	Angle of stator flux vector to the d- axis of the rotor reference frame
ω_{est}	Estimated speed of SyRM
ω_{ref}	Reference speed of SyRM
ω_s and ω_d	Speeds of stator flux vector of stator and the rotor
$\psi_{s\alpha}$ and $\psi_{s\beta}$	Fluxes in orthogonal reference frame
$v_\alpha, v_\beta, i_\alpha$ and i_β	Voltages and current in orthogonal reference frame
S_A, S_B, S_C	Switching signals
v_a, v_b and v_c	Stator voltages
i_a, i_b and i_c	Stator currents
i_d^*, i_q^* and i_d, i_q	d-q axis reference and actual fluxes
ψ_d^*, ψ_q^* and ψ_d, ψ_q	d-q axis reference and actual currents
p	Pole pair
L_d, L_q	Direct and Quardature axis inductances
T_e	Electromagnetic torque
T_L	Pump load torque
R_a	Stator winding resistance of SyRM
I_g	Utility grid current
V_g	Utility grid current
K_{pump}	Pump constant

L_f	Interfacing inductor
N_S, N_P	Numbers of PV modules connected in series and parallel
R_f	Resistance of the R-C ripple filter
S	Solar irradiance
$V_{VSC}, I_{VSC}, VA_{VSC}$	Voltage (V), current (A) and VA (kVA) rating of the VSC
$V_{VSI}, I_{VSI}, VA_{VSI}$	Voltage (V), current (A) and VA (kVA) rating of the VSI